Dynamic Reconstruction and Rendering of 3D Tomosynthesis Images

Johnny Kuo[1*], Peter A. Ringer[1*], Steven G. Fallows[1*],
Predrag R. Bakic[2†], Andrew D. A. Maidment[2†], Susan Ng[1*]

[1] Real-Time Tomography LLC, 1709 Balsam Lane, Villanova, PA, USA 19085
[2] University of Pennsylvania, Dept. of Radiology, 1 Silverstein Building,
3400 Spruce St., Philadelphia, PA, USA 19104

ABSTRACT

Dynamic Reconstruction and Rendering (DRR) is a fast and flexible tomosynthesis image reconstruction and display implementation. By leveraging the computational efficiency gains afforded by off-the-shelf GPU hardware, tomosynthesis reconstruction can be performed on demand at real-time, user-interactive frame rates. Dynamic multiplanar reconstructions allow the user to adjust reconstruction and display parameters interactively, including axial sampling, slice location, plane tilt, magnification, and filter selection. Reconstruction on-demand allows tomosynthesis images to be viewed as true three-dimensional data rather than just a stack of two-dimensional images. The speed and dynamic rendering capabilities of DRR can improve diagnostic accuracy and lead to more efficient clinical workflows.

Keywords: Digital tomosynthesis, real-time reconstruction, dynamic reconstruction and rendering, breast imaging, GPU

1. INTRODUCTION

The current clinical practice of breast cancer detection involves two steps: screening and diagnosis. The dominant screening modality today is mammography, using either screen-film or digital mammography detectors. Screening is generally offered to women as determined by age, menopausal status or genetic predisposition. Screening must be rapid and reasonably inexpensive, possessing high sensitivity and moderate specificity. Women identified at screening as exhibiting signs or symptoms that would be consistent with malignancy are then offered diagnostic imaging. Diagnostic imaging is typically multimodality, and while more time consuming and expensive than screening, it has superior specificity without loss of sensitivity. The intent of diagnostic imaging is to refine the diagnosis of breast cancer so that only a small number of women are required to undergo definitive breast biopsy. While regionally dependent, a rough rule of thumb is that for 1000 women invited to screening, 100 require diagnostic imaging, 10 require biopsy and 4 cancers will be found.

Projection mammography is currently the dominant imaging modality for the detection of occult breast cancer. However, projection mammography is subject to a number of fundamental limitations related to the projection process, whereby 2D images are produced of 3D breast anatomy. Normal tissues separated in space can superimpose in the projection image, resulting in regions of artifactual dense tissue which are visually similar to lesions. Another problem of projection mammograms is that true lesions can be masked by superimposed normal tissue[1-4].

Digital breast tomosynthesis (DBT) is an emerging tomographic imaging modality. In DBT, a number of x-ray projection images (generally from 9 to 48 projections) are acquired over a limited angular range (typically 15° to 60°); these are used to reconstruct tomographic images. Tomosynthesis can mitigate the problems of superposition of non-adjacent tissue (false positive densities) and masking of real lesions observed in projection mammography, while also allowing 3D localization of lesions. Several studies suggest that DBT can provide superior diagnostic accuracy compared to standard digital mammography[1,4-9].

The standard approach to tomosynthesis reconstruction is to perform an offline computation to generate a stack of images. The image stack is typically oriented parallel to the detector plane with each image separated by 1 mm depth

---

[*] {Johnny.Kuo | Peter.Ringer | Steven.Fallows | Susan.Ng} @realtimetomography.com, http://www.realtimetomography.com
[†] {Predrag.Bakic | Andrew.Maidment} @uphs.upenn.edu

increments. The radiologist is then presented this set of images. This approach is similar to that used in the clinical review of computed tomography (CT) images. Unfortunately, in the screening environment, the review of DBT images as an image stack is likely to be time consuming, thus increasing the cost of performing DBT. The question also arises as to what diagnostic step is most appropriate following screening DBT; that is, what distinguishes a screening DBT study from a diagnostic DBT study.

We have developed the method of Dynamic Reconstruction and Rendering (DRR) as a solution to both of these questions. DRR starts from a premise of online, on-demand reconstruction. With DRR, a single tomographic image is reconstructed in real-time to the exact depth, magnification level, and plane orientation specified. The real-time interactive nature of DRR bypasses the post-acquisition offline processing step and allows immediate review of the tomographic images. The ability for real-time interaction with DRR allows the observer to interrogate tomosynthesis data as true 3D data instead of just a stack of 2D images. The on-demand approach of DRR offers a number of advantages in a clinical setting. DRR can provide radiologists with greater abilities to interrogate and interpret the 3D image data for more accurate diagnosis. The on-demand reconstruction allows higher throughput, immediate diagnostic review, and is well-suited to interventional procedures.

In this paper, we describe the method of DRR in more detail, present one possible implementation of DRR, and illustrate the applications and advantages of DRR with phantom and clinical data.

2. METHODS

2.1. Reconstruction

DRR uses a backprojection filtering (BPF) rather than a filtered backprojection (FBP). The BPF approach was chosen to save computation time by performing a single filtering step post-reconstruction rather than pre-filtering each projection image. It also has the additional benefit of facilitating quick filter changes so that the filtering can be dynamically changed to optimize visualization of different tissue type and for viewer preference.

Some preprocessing is done to segment the tissue from air, mask invalid image regions, and thickness equalize each source projection image. These preprocessed images are then loaded into GPU (graphics processing unit) texture memory. To compute the tomosynthesis image, each pixel in the reconstruction plane is mapped to a detector location (i.e. texture coordinate) via the projective geometry[10] relationship dictated by the x-ray source position, reconstruction plane position, and detector location. This projective geometry can be solved by a matrix equation transforming the reconstruction plane position (x, y, z) to texture coordinates (u, v) via projection matrix $\mathbf{A}$:

$$\begin{pmatrix} u \\ v \\ s \end{pmatrix} = \begin{pmatrix} A_{11} & A_{12} & A_{13} & A_{14} \\ A_{21} & A_{22} & A_{23} & A_{24} \\ A_{31} & A_{32} & A_{33} & A_{34} \end{pmatrix} \begin{pmatrix} x \\ y \\ z \\ 1 \end{pmatrix} \tag{1}$$

The values A_{ij} depend on the tomosynthesis geometry. The normalized texture coordinates ($u/s, v/s$) are used to sample the texture and add a pixel value to the backprojection. Interpolation is used in the texture sampling to minimize pixelation and improve image quality in the backprojected image. This process is repeated for each pixel in the reconstruction plane, and for each projection in the acquisition data set to generate the tomosynthesis reconstruction.
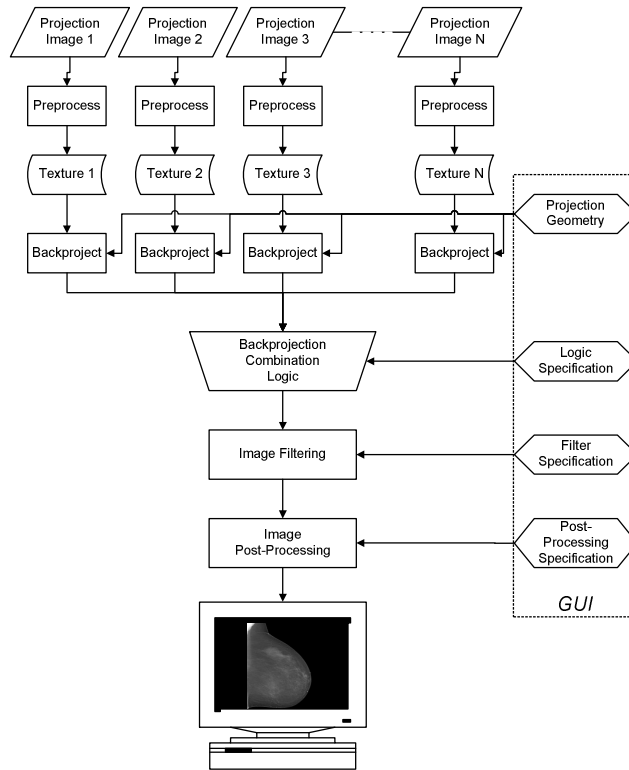
Figure 1: A schematic of the DRR software BPF reconstruction.

Projective transformations are common in computer graphics and can be efficiently computed on a GPU. To speed up the reconstruction to user-interactive frame rates, the reconstruction calculation was parallelized to run on NVIDIA CUDA-enabled GPUs. Modern GPUs have evolved beyond special-purpose fixed function hardware. Current GPUs have programmable hardware which can efficiently execute many simultaneous computations in parallel. This programmable hardware can dramatically speed up floating point computations[11].

The programmable GPU functionality additionally allows for more sophistication to be incorporated into the reconstruction while still maintaining fast reconstruction speeds. Artifact reduction is incorporated directly into the backprojection calculation. With the air segmented from the tissue, the backprojector can ignore computation of pixels in the reconstruction plane if there are air value contributions from any of the source projections. In effect, only the "convex hull" is considered in the reconstruction, which eliminates boundary artifact in the final reconstructed image.
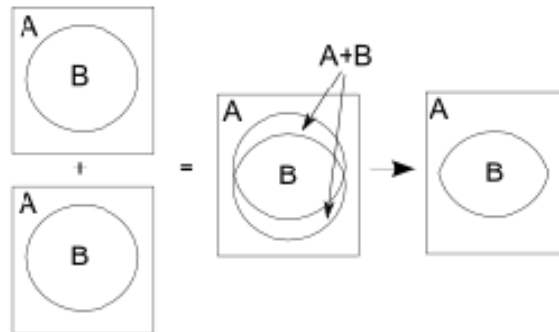

Figure 2: Illustration of the "convex hull." Air pixels (A) can superimpose on body pixels (B) during the backprojection computation. Pixels with both air and body (A+B) contributions are removed and set to air.

The backprojector can also incorporate apodization to reduce visual edge artifacts which occur when summing at image boundaries. When the target anatomy spans the entire detector or abuts a masked invalid region, the backprojection sums contain sharp horizontal edges. These strong edges can result in horizontal line artifacts in the final reconstruction. By implementing the backprojection as a weighted sum, apodization can be used to mitigate this line artifact; image regions including sharp straight line edges can be weighted with a lower factor to smooth out the appearance of the boundary line artifacts.

With backprojection reconstructions, out-of-plane targets blur out since they do not sum coherently. However, dense targets—such as surgical clips, fiducial markers, or calcifications—do not readily blur out in the backprojection reconstruction and can result in out-of-plane object artifact. In the case of bright out-of-plane targets, the non-coherent summation results in object duplication artifact. These out-of-plane object artifacts can be suppressed in the backprojection calculation. Statistical analyses can be used to identify pixels from non-coherently summing targets and remove them from the backprojection sum[12], thereby mitigating artifacts from out-of-plane objects. Importantly, in DRR this out-of-plane artifact suppression can be toggled on and off to allow the radiologist to better determine whether objects visible in the reconstruction are real targets or out-of-plane artifact.

The final step of the reconstruction process is the filtering and post-processing to achieve the final desired image appearance. Performing the filtering once post-reconstruction in a BPF scheme saves significant computation time compared to the typical FBP where pre-filtering is done for each projection. With post-backprojection filtering, fast reconstruction times can be maintained while still allowing dynamically selectable filters. Filters can be selected to enhance visualization of different tissue types (e.g. lesions vs. microcalcifications, or dense vs. fatty tissue), enhance contrast, sharpen the image, and reduce noise.

2.2. Hardware and Software

We have implemented DRR as a fast, flexible, and multiplatform reconstruction engine. A set of sample programs has been developed to demonstrate the interactive reconstruction capabilities of the DRR engine. Reconstruction solutions have been implemented for seven different tomosynthesis system geometries. Six of these geometries were for DBT systems, and one was for a body tomosynthesis system.

The reconstructions were computed on custom workstations built using commercially available, off-the-shelf components. The DRR reconstruction engine has been run on number of different hardware configurations and operating systems during development. The typical development workstation was configured with an Intel Core2 Quad 3.0 GHz processor, 4 GB of RAM, and used Microsoft Windows XP 64-bit. Development primarily targeted Windows XP-64, but the reconstruction engine has also been successfully run on Windows XP 32-bit, Windows Vista, Windows 7, and Linux platforms.

The reconstruction code was developed using NVIDIA CUDA (Compute Unified Device Architecture) libraries on NVIDIA graphics processing units (GPU). The development workstation configurations have run the reconstruction with an NVIDIA GeForce GTX 280, GTX 285, Quadro FX3800, and Quadro FX4800 GPUs. The current prototype demonstration system utilizes an NVIDIA Quadro FX5800 GPU.

2.3. Image Data

Development and testing of the DRR engine was performed using phantom and clinical image data from several sources. Some of the images were obtained from the multimodality breast imaging trial at the University of Pennsylvania (NIH Program Project Grant P01-CA85484). A software breast phantom[13] was also used to validate the geometric accuracy of the reconstruction algorithm[14,15]. Other image data used during the DRR development were vendor-supplied phantom and clinical data.

3. RESULTS

3.1. Reconstruction Speed

The reconstruction frame rate is dependent on several factors including the imaging system geometry, number of projections, projection image size, display monitor resolution (i.e. reconstruction plane resolution), and filtering. Typical reconstruction speeds on the demonstration workstation rendering to a 3 megapixel monitor ranged from 15 to 25 frames per second.

3.2. Magnification and Super-resolution

Conventional magnified views increase the image size via interpolation, which adds no spatial information and does not really improve image quality. While validating the geometric accuracy of the DRR reconstruction[14], it was noted that the accuracy of reconstructed magnified views was greater than the detector resolution. The DRR tomosynthesis reconstructions can provide super-resolution beyond the 2D resolution of the detector[16]. Due to super-resolution, dynamically reconstructing magnified views to full resolution gives sharper images than using interpolation of a pre-reconstructed image (see Figure 3).
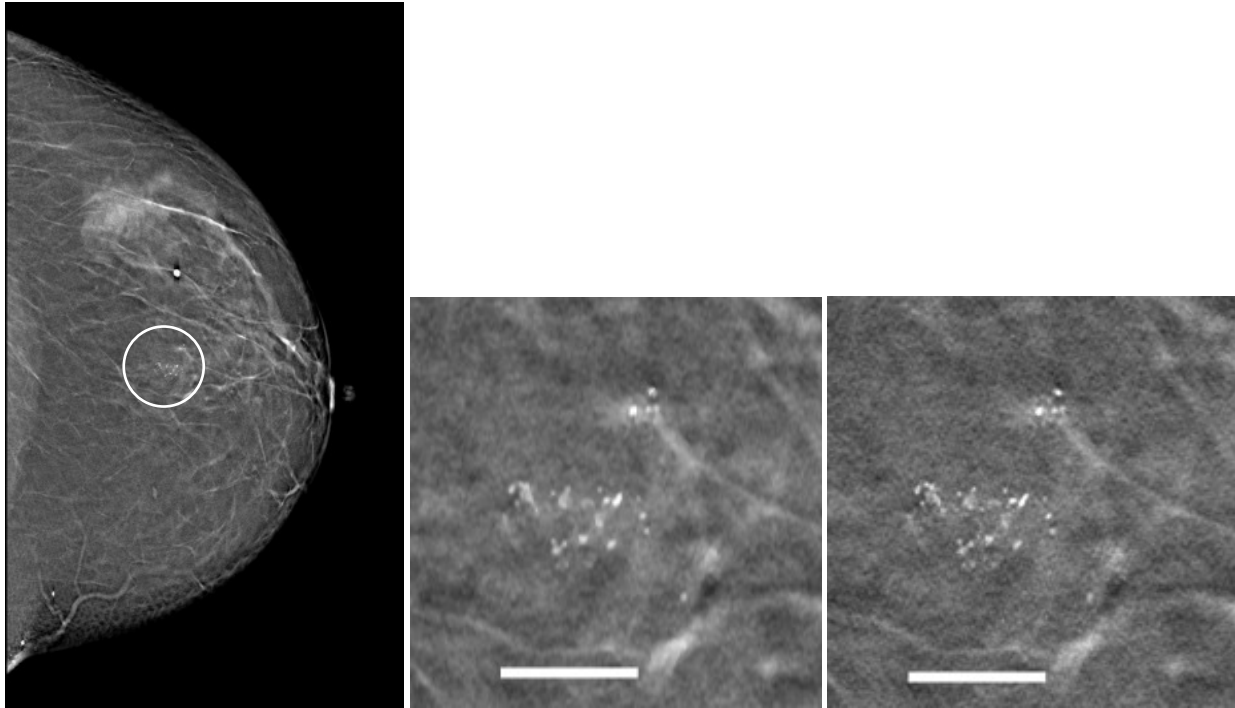
Figure 3: A cluster of microcalcifications is located in DBT Image (left). A conventional interpolated magnified view (middle) of the calcifications makes the image larger without adding image quality. The DRR magnification (right) reconstructs at the full resolution of the magnified view; DRR adds image quality due to super-resolution and gives a sharper, higher resolution image of the calcification cluster.

3.3. Convex Hull Reconstruction

Using a simple backprojection, there are regions in the reconstructed image near the breast-air boundary where varying combinations of air and tissue values contribute to the backprojection sum. These regions cause the appearance of false boundaries in the reconstructed image. By ignoring pixels with any air value contributions, only the convex hull is reconstructed and the false boundaries are eliminated (Figure 4).
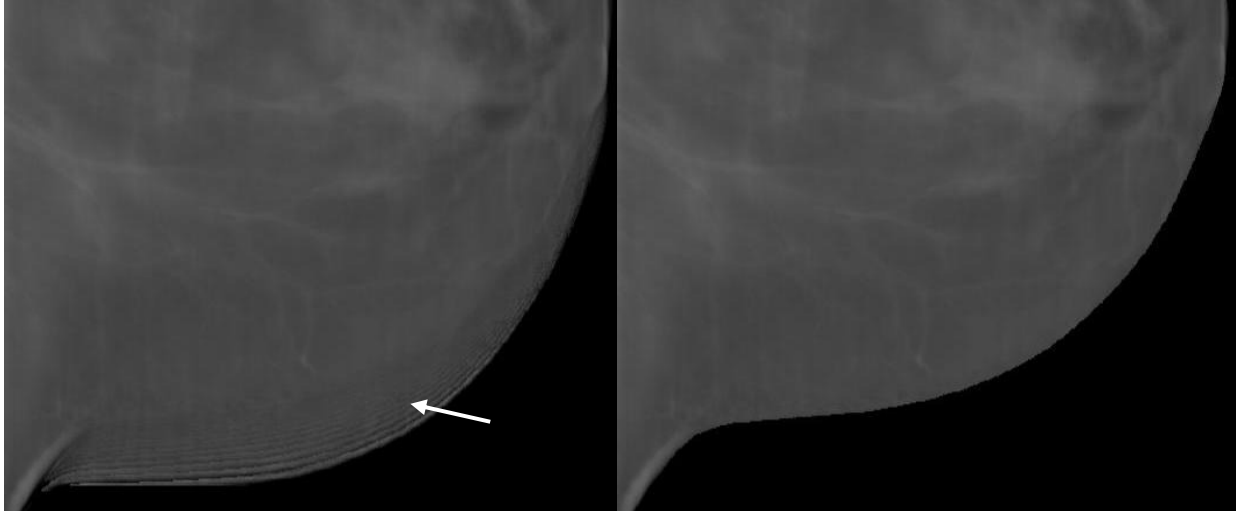
Figure 4: Reconstructions of the same image with a simple backprojection (left) and a convex hull backprojection (right). The dark rings in the duplicate boundary artifact result from darker edge pixels from one projection superimposing on pixels further from the breast boundary on other projections. The convex hull removes boundary duplication artifact.

3.4. Apodization

Portions of the reconstructed image can include boundaries of the projection images (where the imaged anatomy spans the entire width of the detector), or the reconstructed image region may map to an area abutting an invalid region (e.g. where an invalid target like a collimator is masked from the projection image). In either of these cases, the backprojection sum will involve non-overlapping image regions across a strong horizontal edge. This can result in visible horizontal line artifacts in the reconstructed tomosynthesis image. By apodizing the boundary edges, the horizontal edge artifacts can be suppressed (Figure 5).

The conspicuity of the line artifacts and ability of apodization to mitigate these artifacts depends on the number of projection images and the pixel intensity next to the horizontal edge. In general, the line artifact is more prevalent in datasets with fewer projections since the fractional signal contributed by each projection to the backprojection sum is greater. Higher pixel values near the horizontal edge also result in more visible artifacts; the higher pixel values cause a larger difference in values across the boundary, which results in a stronger edge in the backprojection sum. Apodization suppresses these line artifacts, but strong edge artifacts may not be completely eliminated.
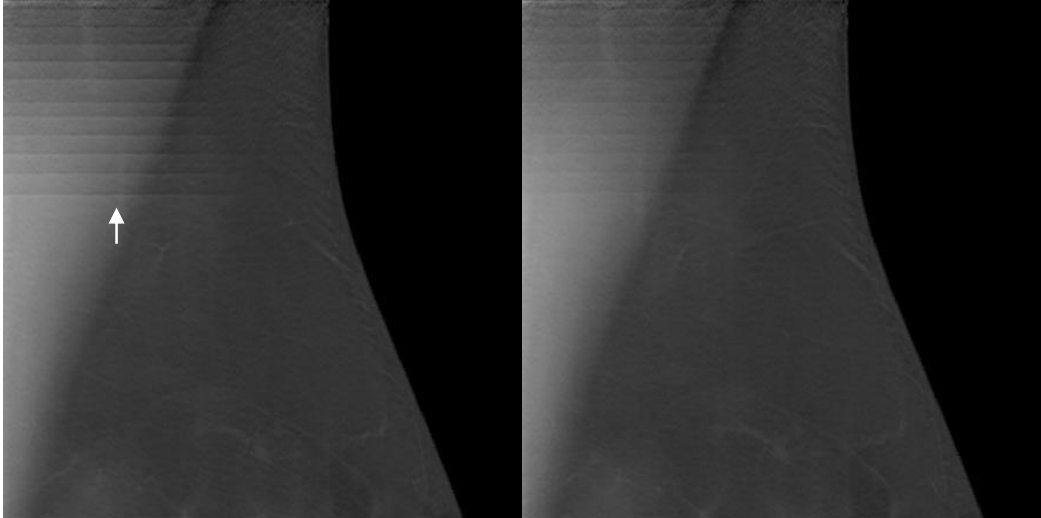
Figure 5: Reconstructed tomosynthesis image without (left) apodization shows noticeable horizontal line artifacts from projection image boundaries. With apodization (right), the horizontal line artifacts are suppressed.

3.5. Artifact Reduction

Bright, out-of-plane targets can introduce object duplication artifact. These out of plane targets sum non-coherently in the backprojection. By identifying pixels from non-coherently summing targets, DRR can remove these out-of-focus target contributions from the backprojection sum and reduce artifacts in the final reconstruction (Figure 6). In general, small out-of-plane targets like microcalcifications, small surgical clips, and small fiducial markers are more effectively suppressed. Larger objects tend to overlap over larger depth ranges in the backprojection, which makes it more difficult to ascertain whether they are summing coherently or not.
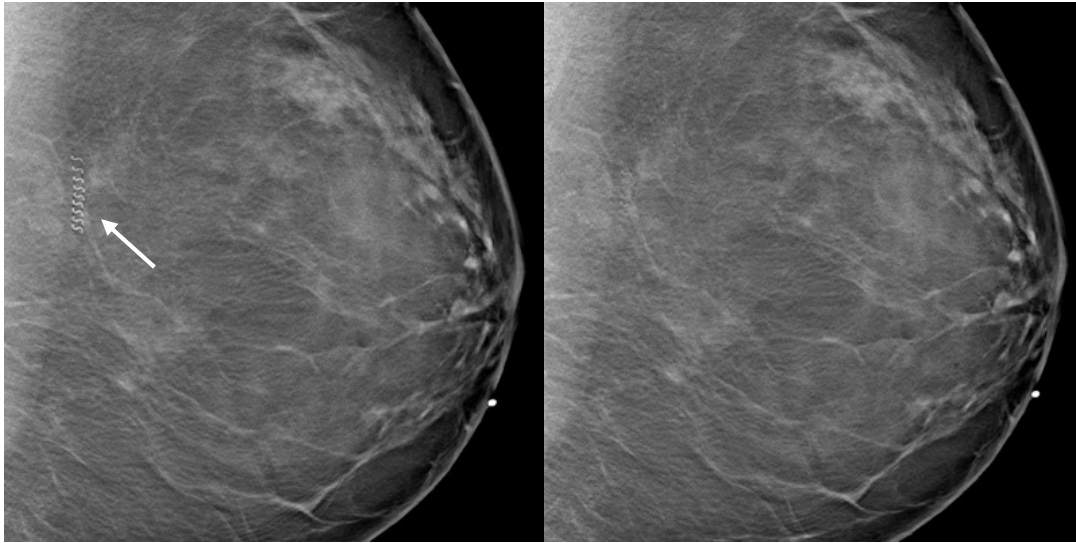
Figure 6: At left, the reconstructed image is shown outside the focal plane of the surgical clip. At right, the artifacts from the out-of-plane surgical clip have been eliminated by enabling the artifact reduction DRR filter.

3.6. Oblique Reconstructions

On-demand reconstruction allows interactive tilting of the reconstruction plane to better visualize anatomy which is not parallel to detector. Examples of such anatomy from breast imaging include vessels (Figure 7) or calcification clusters. There are scanner geometry-dependent limits to how much the tomosynthesis reconstruction plane can be angled. The limited scan angle of tomosynthesis results in anisotropic resolution and incomplete spatial information in the axial direction. Angled multiplanar views are not possible with a static stack of pre-reconstructed images.
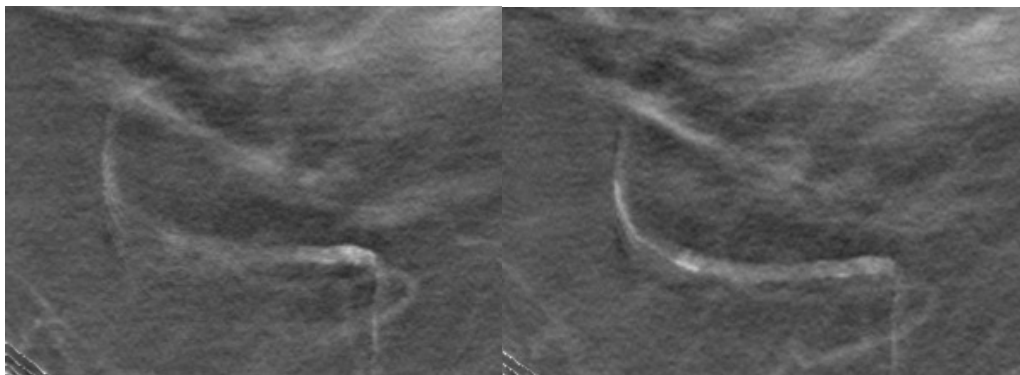
Figure 7: Calcified vessel shown with the reconstructed plane parallel (left) and tilted 2° (right) relative to the detector plane. The vessel is better visualized from the angled view.

4. DISCUSSION

Digital breast tomosynthesis (DBT) overcomes many of the limitations of projection mammography and shows promise as a breast cancer screening modality. As with any other new technology, there are a number of challenges to overcome for widespread deployment of DBT. One major challenge is that DBT generates approximately 50 times more images than projection mammography. Current recommendations by DBT manufacturers to reconstruct images in 1mm slice increments translate into 30 to 100 images per DBT exam. Using a mammography workflow model with the large number of DBT images will dramatically increase radiologists' workloads and make DBT impractical. DBT cannot be viewed as a series of 2D images if it is to become clinically viable.

The premise of Dynamic Reconstruction and Rendering (DRR) has been to approach DBT using real-time interactions with the imaging data, more akin to how ultrasound is used for real-time imaging or how radiologists can dynamically view volumetric CT data. Rather than reconstruct an entire stack of image slices, a single cross-sectional plane is reconstructed on-demand. Dynamic reconstruction offers the ability to examine any slice depth, tilt the reconstruction plane for multiplanar views, and give higher resolution magnifications. This interactive flexibility allows DRR to interrogate the tomosynthesis dataset as true 3D data rather than a static stack of 2D images.

To achieve the computational speed necessary for on-demand reconstruction, our implementation of DRR uses a backprojection filtering (BPF) scheme rather than the traditional filtered backprojection (FBP). Backprojection and filtering are both linear operations; it is numerically equivalent to filter the images before or after backprojection and summation[17]. We have verified this equivalence with our own experiments, and others have also shown that post-backprojection filtering gives functionally equivalent images to pre-backprojection filtering at significantly reduced computational cost[18,19].

Combining BPF with the acceleration from the GPU implementation boosts the computation speed enough for dynamic, on-demand reconstruction. The on-demand reconstruction from DRR offers dynamic flexibility which is not readily achievable with the standard pre-reconstructed 1mm slice stack. With static slices, small targets located between the pre-reconstructed slices will be blurred. The amount of blurring from being out of plane will vary depending on the system geometry, but the blurring can be significant. Bakic, *et al* found in a DBT geometric accuracy study that fiducial size estimates had a 50% error when the marker was 0.6mm away from the plane of focus[14]. Just viewing static slices, the radiologist can potentially miss small targets, like microcalcifications, which may be blurred from being positioned between the fixed pre-reconstructed slices. With on-demand reconstruction, the reconstruction plane can be placed at an exact depth position to achieve the best focus of the target anatomy.

Another benefit of DRR is that magnifications generate reconstructed images at full resolution rather than interpolating a pre-reconstructed image. Magnification via interpolation provides no real improvement in image quality. DRR takes advantage of tomographic super-resolution[16], whereby the multiple projection images allow reconstruction to a finer effective spatial resolution than the detector element spacing. DRR provides a unique reconstruction for every magnification at the full resolution of the displayed region of interest. Consequently, DRR can utilize super-resolution to reconstruct magnified views with a higher level of detail for enhanced viewing of fine structures.

DRR allows interactive tilting of the reconstruction plane. The angled multiplanar views enable better visualization of complex 3D targets which may not be oriented parallel to the detector plane. There are system limits to how much the reconstruction plane can be tilted. Tomosynthesis has anisotropic spatial resolution due to its limited angular range of acquisition. The axial dimension typically contains incomplete spatial information and has poorer resolution. Conventional wisdom restricts the reconstruction plane tilt to the acquisition scan angle. However, preliminary research from the University of Pennsylvania suggests that the there is usable spatial information well beyond the tomosynthesis scan angle[20].

Visualization in digital images is greatly dependent on the image processing algorithms used to present the images; consequently, image processing algorithms can significantly affect the diagnostic outcome. In CT, images are reconstructed with multiple reconstruction filters (e.g. for bone and soft tissue). In a recent retrospective study for the Digital Mammography Imaging Screening Trial (DMIST), it was found that the visibility of lesions was influenced by image contrast, therefore by the image processing algorithm[21]. Other studies quantifying the effect image processing

Proc. of SPIE Vol. 7961 796116-8

Downloaded From: http://spiedigitallibrary.org/ on 07/15/2016 Terms of Use: http://spiedigitallibrary.org/ss/TermsOfUse.aspx

4. DISCUSSION

Digital breast tomosynthesis (DBT) overcomes many of the limitations of projection mammography and shows promise as a breast cancer screening modality. As with any other new technology, there are a number of challenges to overcome for widespread deployment of DBT. One major challenge is that DBT generates approximately 50 times more images than projection mammography. Current recommendations by DBT manufacturers to reconstruct images in 1mm slice increments translate into 30 to 100 images per DBT exam. Using a mammography workflow model with the large number of DBT images will dramatically increase radiologists' workloads and make DBT impractical. DBT cannot be viewed as a series of 2D images if it is to become clinically viable.

The premise of Dynamic Reconstruction and Rendering (DRR) has been to approach DBT using real-time interactions with the imaging data, more akin to how ultrasound is used for real-time imaging or how radiologists can dynamically view volumetric CT data. Rather than reconstruct an entire stack of image slices, a single cross-sectional plane is reconstructed on-demand. Dynamic reconstruction offers the ability to examine any slice depth, tilt the reconstruction plane for multiplanar views, and give higher resolution magnifications. This interactive flexibility allows DRR to interrogate the tomosynthesis dataset as true 3D data rather than a static stack of 2D images.

To achieve the computational speed necessary for on-demand reconstruction, our implementation of DRR uses a backprojection filtering (BPF) scheme rather than the traditional filtered backprojection (FBP). Backprojection and filtering are both linear operations; it is numerically equivalent to filter the images before or after backprojection and summation[17]. We have verified this equivalence with our own experiments, and others have also shown that post-backprojection filtering gives functionally equivalent images to pre-backprojection filtering at significantly reduced computational cost[18,19].

Combining BPF with the acceleration from the GPU implementation boosts the computation speed enough for dynamic, on-demand reconstruction. The on-demand reconstruction from DRR offers dynamic flexibility which is not readily achievable with the standard pre-reconstructed 1mm slice stack. With static slices, small targets located between the pre-reconstructed slices will be blurred. The amount of blurring from being out of plane will vary depending on the system geometry, but the blurring can be significant. Bakic, *et al* found in a DBT geometric accuracy study that fiducial size estimates had a 50% error when the marker was 0.6mm away from the plane of focus[14]. Just viewing static slices, the radiologist can potentially miss small targets, like microcalcifications, which may be blurred from being positioned between the fixed pre-reconstructed slices. With on-demand reconstruction, the reconstruction plane can be placed at an exact depth position to achieve the best focus of the target anatomy.

Another benefit of DRR is that magnifications generate reconstructed images at full resolution rather than interpolating a pre-reconstructed image. Magnification via interpolation provides no real improvement in image quality. DRR takes advantage of tomographic super-resolution[16], whereby the multiple projection images allow reconstruction to a finer effective spatial resolution than the detector element spacing. DRR provides a unique reconstruction for every magnification at the full resolution of the displayed region of interest. Consequently, DRR can utilize super-resolution to reconstruct magnified views with a higher level of detail for enhanced viewing of fine structures.

DRR allows interactive tilting of the reconstruction plane. The angled multiplanar views enable better visualization of complex 3D targets which may not be oriented parallel to the detector plane. There are system limits to how much the reconstruction plane can be tilted. Tomosynthesis has anisotropic spatial resolution due to its limited angular range of acquisition. The axial dimension typically contains incomplete spatial information and has poorer resolution. Conventional wisdom restricts the reconstruction plane tilt to the acquisition scan angle. However, preliminary research from the University of Pennsylvania suggests that the there is usable spatial information well beyond the tomosynthesis scan angle[20].

Visualization in digital images is greatly dependent on the image processing algorithms used to present the images; consequently, image processing algorithms can significantly affect the diagnostic outcome. In CT, images are reconstructed with multiple reconstruction filters (e.g. for bone and soft tissue). In a recent retrospective study for the Digital Mammography Imaging Screening Trial (DMIST), it was found that the visibility of lesions was influenced by image contrast, therefore by the image processing algorithm[21]. Other studies quantifying the effect image processing

algorithms in digital mammograms have also found that the variability between different manufacturer-recommended or default image processing algorithms significantly impacted the detection of lesions[22,23]. It logically follows that DBT would also benefit from having several filters tuned to optimally display different tissue types. Since there is a single post-backprojection filtering step, DRR has the ability to use dynamically selectable filters while maintaining user interactive display speeds. The online dynamic reconstruction allows easy substitution of filters to enhance visibility of calcifications vs. lesions or to better enhance dense vs. fatty tissue.

DRR was designed with the clinical environment in mind. In a screening context, faster examination and reading times are desirable. Since DRR obviates the offline processing step, there is no offline processing delay before the images are available for viewing. This allows the technologist to check the tomosynthesis images immediately post-acquisition to assess whether re-imaging is necessary due to patient motion or poor patient positioning. When used for diagnosis, the interactive flexibility of DRR provides the radiologist with more complete 3D information. The radiologist can interrogate the image data more carefully by advancing the reconstruction plane at increments finer than the standard 1mm slice spacing. Multiplanar viewing allows the radiologist to angle the reconstruction plane to better visualize the 3D morphology of the imaged anatomy. Perhaps most importantly, the radiologist can dynamically magnify the tomosynthesis image and take advantage of the greater detail afforded by super-resolution.

The described DRR implementation performs at interactive frame rates using off-the-shelf hardware. In general, video frame rates (24-30 frames/sec) are considered the minimum to be real-time. A minimum of 15 frames/sec is the approximate lower bound for effective interaction[24]. The DRR implementation is currently capable of achieving user interactive speeds using a 3 megapixel monitor. The final frame rate depends on the tomosynthesis system geometry, number of projections, display resolution, and processing enabled. In a worst case scenario of complicated geometry, numerous projections, high resolution, and enabling of all filtering and processing options, reconstruction speed can drop below the interactive frame rate threshold. However, the described DRR implementation was developed and tested on previous generation GPU hardware. Current generation GPUs should be faster. In the last several years, GPU computational power has increased at a rate exceeding Moore's Law[25]. With the rapidly advancing GPU performance (and decreasing cost for performance) coupled with the advantages of dynamic reconstruction, it is easy to envision on-demand, interactive reconstruction becoming the standard approach for digital tomosynthesis imaging.

5. CONCLUSION

The real-time nature of DRR gives the user a flexible and powerful tool to interrogate the tomosynthesis data. DRR has significant advantages to the conventional approach of reconstructing fixed 1mm spaced slices. Using commercially available, off-the-shelf GPU hardware, DRR can place the reconstruction plane at exact depths for optimum small target focus, utilize angled multiplanar views for better 3D visualization, and use super-resolution to add finer spatial resolution to magnified views. The fast on-demand reconstruction can potentially speed up clinical workflows, and the interactive reconstruction provides more complete information for improved diagnostic accuracy.

6. ACKNOWLEDGEMENTS

REFERENCES

[1] Elizabeth A. Rafferty, L. Niklason, and E. Halpern, "Assessing Radiologist Performance Using Combined Full-Field Digital Mammography and Breast Tomosynthesis Versus Full-Field Digital Mammography Alone: Results of a Multi-Center, Multi-Reader Trial," in *93rd Scientific Assembly and Annual Meeting of the RSNA* (2007).

[2] H. J. Teertstra, C. E. Loo, M. A. A. J. Bosch, H. Tinteren, E. J. T. Rutgers, S. H. Muller, and K. G. A. Gilhuijs, "Breast tomosynthesis in clinical practice: initial results," *Eur Radiol* **20**, 16-24 (2009) [doi:10.1007/s00330-009-1523-2].

[3] J. Eberhard, D. Albagli, A. Schmitz, B. Claus, P. Carson, M. Goodsitt, H. Chan, M. Roubidoux, J. Thomas, et al., "Mammography Tomosynthesis System for High Performance 3D Imaging," in *Digital Mammography* **4046**, pp. 137-143, Springer Berlin / Heidelberg (2006).

[4] S. P. Poplack, T. D. Tosteson, C. A. Kogel, and H. M. Nagy, "Digital breast tomosynthesis: initial experience in 98 women with abnormal digital screening mammography," *AJR Am J Roentgenol* **189**, 616-623 (2007) [doi:10.2214/AJR.07.2231].

[5] I. Andersson, D. Ikeda, S. Zackrisson, M. Ruschin, T. Svahn, P. Timberg, and A. Tingberg, "Breast tomosynthesis and digital mammography: a comparison of breast cancer visibility and BIRADS classification in a population of cancers with subtle mammographic findings," *European Radiology* **18**, 2817-2825 (2008).

[6] M. J. Michell, R. K. Wasan, P. Whelehan, A. Iqbal, C. P. Lawinski, A. N. Donaldson, D. R. Evans, C. Peacock, and A. R. M. Wilson, "Digital breast tomosynthesis: a comparison of the accuracy of digital breast tomosynthesis, two-dimensional digital mammography and two-dimensional screening mammography (film-screen)," *Breast Cancer Research* **11**, O1 (2009).

[7] D. Gur, G. S. Abrams, D. M. Chough, M. A. Ganott, C. M. Hakim, R. L. Perrin, G. Y. Rathfon, J. H. Sumkin, M. L. Zuley, et al., "Digital breast tomosynthesis: observer performance study," *AJR Am J Roentgenol* **193**, 586-591 (2009) [doi:10.2214/AJR.08.2031].

[8] M. J. Michell, R. K. Wasan, A. Iqbal, C. Peacock, D. R. Evans, and J. C. Morel, "Two-view 2D digital mammography versus one-view digital breast tomosynthesis," *Breast Cancer Research* **12**, P3 (2010).

[9] G. Gennaro, A. Toledano, C. di Maggio, E. Baldan, E. Bezzon, M. La Grassa, L. Pescarini, I. Polico, A. Proietti, et al., "Digital breast tomosynthesis versus digital mammography: a clinical performance study," *European Radiology* **20**, 1545-1553 (2010).

[10] Paul Haeberli and Mark Segal, "Texture mapping as a fundamental drawing primitive," in *Eurographics*, pp. 259-266, Paris, France (1993).

[11] M. Harris, "Many-core GPU computing with NVIDIA CUDA," in *Proceedings of the 22nd annual international conference on Supercomputing*, pp. 1–1, ACM, New York, NY, USA (2008) [doi:10.1145/1375527.1375528].

[12] T. Wu, R. H. Moore, and D. B. Kopans, "Voting strategy for artifact reduction in digital breast tomosynthesis," *Med. Phys.* **33**, 2461 (2006) [doi:10.1118/1.2207127].

[13] C. Zhang, P. R. Bakic, and A. D. A. Maidment, "Development of an anthropomorphic breast software phantom based on region growing algorithm," in *Proceedings of SPIE*, pp. 69180V-69180V-10, San Diego, CA, USA (2008) [doi:10.1117/12.773011].

[14] Predrag R. Bakic, Peter Ringer, Johnny Kuo, Susan Ng, and Andrew D.A. Maidment, "Analysis of Geometric Accuracy in Digital Breast Tomosynthesis Reconstruction," *Digital Mammography* **6136**, 62-69 (2010).

[15] P. R. Bakic, S. Ng, P. Ringer, A. Carton, E. F. Conant, and A. D. A. Maidment, "Validation and optimization of digital breast tomosynthesis reconstruction using an anthropomorphic software breast phantom," presented at Medical Imaging 2010: Physics of Medical Imaging, 2010, San Diego, California, USA, 76220F-76220F-9 [doi:10.1117/12.845299].

[16] Raymond J. Acciavatti and Andrew D.A. Maidment, "Investigating the potential for super-resolution in digital breast tomosynthesis," in *SPIE Medical Imaging* (2011).

[17] G. T. Herman, *Image Reconstruction from Projections: The Fundamentals of Computerized Tomography*, Academic Pr (1980).

[18] B. Zhang and G. L. Zeng, "An immediate after-backprojection filtering method with blob-shaped window functions for voxel-based iterative reconstruction," *Phys Med Biol* **51**, 5825-5842 (2006) [doi:10.1088/0031-9155/51/22/007].

[19] S. Suzuki and S. Yamaguchi, "Comparison between an image reconstruction method of filtering backprojection and the filtered backprojection method," *Appl. Opt.* **27**, 2867-2870 (1988) [doi:10.1364/AO.27.002867].

[20] R. J. Acciavatti and A. D. Maidment, "An Analysis of Super-Resolution in Oblique Reconstructions for Digital

Breast Tomosynthesis," presented at DOD Era of Hope, August 2011.

[21] E. D. Pisano, S. Acharyya, E. B. Cole, H. S. Marques, M. J. Yaffe, M. Blevins, E. F. Conant, R. E. Hendrick, J. K. Baum, et al., "Cancer cases from ACRIN digital mammographic imaging screening trial: radiologist analysis with use of a logistic regression model," *Radiology* **252**, 348-357 (2009) [doi:10.1148/radiol.2522081457].

[22] E. B. Cole, E. D. Pisano, D. Zeng, K. Muller, S. R. Aylward, S. Park, C. Kuzmiak, M. Koomen, D. Pavic, et al., "The Effects of Gray Scale Image Processing on Digital Mammography Interpretation Performance1," *Academic Radiology* **12**, 585-595 (2005) [doi:doi: DOI: 10.1016/j.acra.2005.01.017].

[23] F. Zanca, J. Jacobs, C. Van Ongeval, F. Claus, V. Celis, C. Geniets, V. Provost, H. Pauwels, G. Marchal, et al., "Evaluation of clinical image processing algorithms used in digital in digital mammography," *Med Phys* **36**, 765-775 (2009).

[24] M. Reddy, "The Effects of Low Frame Rate on a Measure for User Performance in Virtual Environments," Technical Report ECS-CSG-36-97, University of Edinburgh (1997).

[25] John Owens, "GPUs: Engines for Future High-Performance Computing," in *HPEC 2004 Proceedings* (2004).